AGNES in irreversible systems

Josep Galceran, Encarna Companys, Jaume Puy, Jose Paulo Pinheiro, Elise Rotureau

Journal of Electroanalytical Chemistry 901 (2021) 115750

Contents lists available at ScienceDirect

Journal of Electroanalytical Chemistry

journal homepage: www.elsevier.com/locate/jelechem

AGNES in irreversible systems: The indium case

Josep Galceran [a,*], Encarna Companys [a], Jaume Puy [a], Jose Paulo Pinheiro [b], Elise Rotureau [b]

[a] Departament de Química. Universitat de Lleida, and AGROTECNIO-CERCA, Rovira Roure 191, 25198 Lleida, Catalonia, Spain
[b] CNRS, LIEC (Laboratoire Interdisciplinaire des Environnements Continentaux), UMR7360, Vandoeuvre-lès-Nancy F54501, France

ARTICLE INFO

Keywords:
Speciation
AGNES
SSCP
Irreversibility
Indium
Complexation
Pseudopolarograpy
Potentiometric stripping analysis

ABSTRACT

Free indium concentrations can be determined using AGNES (Absence of Gradients and Nernstian Equilibrium Stripping) with no relevant hindrance from the irreversibility of the In^{3+}/In° redox couple at a mercury electrode. The electroactivity, high lability and mobility of the In hydroxy species help in reaching AGNES conditions for a relatively moderate ratio (deposition time):(gain), which decreases with increasing pH due to the growing contribution of the hydroxy species. In the related technique SSCP (Scanned Stripping ChronoPotentiometry), points corresponding to more positive deposition potentials are said to be "at the foot of the wave". Some of these points can reach equilibrium along the fixed SSCP deposition time, so that these points are effectively AGNES experiments, and free metal ion concentrations (such as those of free indium) can also be computed from them provided sufficiently accurate data are available. A new representation of the SSCP wave allows for the diagnosis of the potential region where AGNES conditions are fulfilled.

1. Introduction

Absence of Gradients and Nernstian Equilibrium Stripping (AGNES) is an electroanalytical technique that typically quantifies the concentration of free metal ions in solution [1,2]. The fundamentals of AGNES are quite similar to those of an ion selective electrode (ISE), since the main requirement is the attainment of Nernstian equilibrium at the interphase solution/electrode. Nevertheless, the nature of the reactions involved when using AGNES and an ISE are rather different, leading to different approaches to ascertain equilibrium and, thus, validating the use of these techniques. In AGNES, the accumulated reduced element in the electrode has to reach Nernstian equilibrium with ions in solution by the end of the deposition stage (or first stage), which typically is of the order of hundreds of seconds, in a sufficient amount to be comfortably quantified in the stripping stage (or second stage).

AGNES has been successfully implemented for divalent cations such as Zn^{2+}, Cd^{2+} and Pb^{2+} [3–6], whose reduced forms amalgamate in a mercury electrode. The free concentration of Cu^{2+} could also be measured with gold electrodes [7]. More recently, AGNES has been extended beyond divalent analytes, such as antimony hydroxide [8] and the free (i.e. hexaaquo) ionic form of Indium (III) [9–11].

Indeed, due to its high solubility in mercury and its negative standard redox potential, indium is suitable for the application of AGNES. The indium case is very interesting, since there are more than one electroactive species (In^{3+}, $In(OH)^{2+}$,$In(OH)_2^{+}$) [12–14] that exhibit different degrees of reversibility. Since AGNES is an equilibrium technique, it means that upon reaching the target equilibrium, the reduced amount will be proportional to each one of the indium species in solution, and accordingly to the free indium concentration [In^{3+}]. The time needed to attain AGNES conditions implicitly depends (among other factors) on the interplay between the electrodic reduction reaction at the electrode/solution interface and the kinetics of the (de)hydration and/or (de)protonation reactions of indium species in solution. Regardless of the dynamics of reactions leading to the metal accumulation in the electrode, equilibrium time can be simply established by time-course experiments (or AGNES trajectories) for any required deposition potential.

From the interpretation of data obtained with the related technique SSCP (Scanned Stripping ChronoPotentiometry), the question arose whether AGNES could, perhaps, encounter some difficulties with indium, given the irreversibility of the redox couple In^{3+}/In° [14,15].

The aim of this work is to consider the impact of indium electrochemical irreversibility on AGNES (at different pH values, with different proportions between free indium and its hydrolysis products) and provide tools for the visualization and interpretation of a region in the foot of an SSCP wave as AGNES-like experiments (which applied to indium solutions additionally show that indium irreversibility is overcome).

* Corresponding author.
E-mail address: josep.galceran@udl.cat (J. Galceran).

https://doi.org/10.1016/j.jelechem.2021.115750
Received 1 July 2021; Received in revised form 28 September 2021; Accepted 30 September 2021
Available online 6 October 2021

2. Principles of the techniques

2.1. AGNES

The key idea of AGNES is the accumulation of the analyte (in a first deposition stage) until a special situation of equilibrium is reached: a) absence of gradients in the concentration profiles and b) Nernstian equilibrium at the electrode interface. The deposition time is not fixed *a priori*, but adjusted until the equilibrium is successfully checked (e.g. confirming no variation in the analytical response despite a relevant increase in the deposition time). Due to the sought Nernstian equilibrium, it is very useful to work with *Y*, the gain (or pre-concentration factor):

$$Y = \frac{[In^0]}{[In^{3+}]} = \exp\left[-\frac{3F}{RT}\left(E_1 - E^{0'}\right)\right] \quad (1)$$

where E_1 is the deposition potential and $E^{0\prime}$ the formal standard potential. *F* is the Faraday constant; *R*, the gas constant; and *T*, the temperature.

The amount of accumulated analyte is quantified in the second stage of AGNES. When the stripped charge is taken as the analytical signal, from Faraday's law, it follows

$$Q = Y\eta_Q[In^{3+}] \quad (2)$$

with

$$\eta_Q = 3\ F\ V \quad (3)$$

where *V* is the volume of the mercury electrode and the number 3 (number of exchanged electrons) holds for the trivalent indium case.

In the case of indium, to avoid the impact of its irreversibility on short-timescale techniques such as Differential Pulse Polarography [10], the gain is found from a calibration. This calibration is usually run at a sufficiently low pH, so that the free indium concentration (given by a speciation code such as Visual Minteq) is practically the total one, with small practical impact from the specific set of constants assumed.

In AGNES practice, the attainment of equilibrium is confirmed by the plateau in a trajectory (e.g. *Q* vs. deposition time, t_1, in various AGNES experiments) and by the use of more than one gain.

A special feature of the In system is the presence of the indium hydroxy complexes which are also electroactive [14]. Thus, the accumulation of In° in the amalgam can proceed from the reduction of the free indium and/or from the direct reduction of the hydroxy species for convenient deposition potentials.

2.2. SSCP

An SCP (stripping chronopotentiometry, also known as Potentiometry Stripping Analysis [16,17]) experiment [18] consists in a first stage at a given deposition potential E_d during a deposition time t_d, that accumulates reduced metal (In° in our case) in the amalgam, followed by a stripping stage where the accumulated In° is reoxidized. The reoxidation is driven by a fixed stripping current I_S. The time needed until full depletion of In° from the amalgam is called transition time τ and is obtained from the recording of the potential along the stripping stage. The stripped charge of an SCP experiment can be computed from the measured transition time as

$$Q = (I_s - I_{Ox})\tau \approx I_s\tau \quad (4)$$

where I_{Ox} is the oxygen current [19]. In some cases, it can be checked (or assumed) that $I_{Ox} \ll I_s$.

An SSCP wave gathers the transition times for a collection of SCP experiments with the same deposition time (t_d), but each SCP experiment with a different E_d [20,21]. At sufficiently negative deposition potentials, diffusion-limited conditions are reached, the deposition current I_d reaches its maximum value (in absolute value) I_d^* and the transition time also reaches its maximum value τ*.

The SSCP technique is a kind of pseudopolarography [22,23], because it also collects responses of a stripping method at varying deposition potentials. One relevant feature is that SCP with full depletion of the analyte from the amalgam allows for a direct quantification of the accumulated charge in the deposition stage, which is not always the case in other stripping methods (e.g. in Differential Pulse-Anodic Stripping Voltammograms) when dealing with complex media.

In planar or spherical geometry under excess of ligand conditions, the steady-state *diffusion-limited* SSCP current I_d^* in an indium solution can be written as.

$$I_d^* = 3FAD_{In^{3+}}\frac{[In^{3+}](1+\varepsilon K')}{\delta} \quad (5)$$

where we have also assumed –for the sake of simplicity- that all complexes (including hydroxy species) are fully labile [14] and that they all share a common normalized diffusion coefficient (with respect to that of In^{3+}),

$$\varepsilon = \frac{D_{InOH^{2+}}}{D_{In^{3+}}} = \frac{D_{In(OH)_2^+}}{D_{In^{3+}}} = \frac{D_{In(OH)_3}}{D_{In^{3+}}} \quad (6)$$

Any irreversibility of the $In^{3+}/In°$ redox couple disappears due to the large overvoltage in diffusion-limited conditions. *A* stands for the electrode area, δ for the effective diffusion layer and K' for the global conditional stability constant (in excess ligand conditions), which for indium hydroxy species reads

$$K' \equiv \frac{\sum_{n=1}^{nmax}[In(OH)_n]}{[In^{3+}]} \quad (7)$$

a value pH-dependent.

In SSCP, the Nernstian relationship is typically written as

$$\theta = \exp\left[\frac{3F}{RT}\left(E_1 - E^{0'}\right)\right] = \frac{1}{Y} \quad (8)$$

which can be identified as the reciprocal of the (AGNES) gain *Y*, see Eq. (1).

A useful parameter (function of the potential, via θ) in SSCP is the characteristic deposition time τ_d (see Eq. (11), below). For the case of a fully reversible redox couple in a solution with fully labile complexes under ligand excess conditions

$$\tau_d = \frac{V\delta}{AD_M(1+\varepsilon K')\theta} \quad (9)$$

The factor $(1 + \varepsilon K')$ becomes $(1 + K')$ if the hydroxy species have the same mobility as the free metal ($\varepsilon = 1$). The factor $(1 + K')$ was missing in Eq. (15) of ref. [20], in Eq. (6) of ref. [21] and in Eq. (14) of ref. [24] which should have read (in their notation):

$$\tau_d = \frac{V\left(1/\bar{\delta}_M + 1/r_0\right)^{-1}}{A\bar{D}(1+K')\theta} \quad (10)$$

Eq. (10) is consistent with the reported expression just below Eq. (7) in ref. [25]. See section "SSCP model for reversible redox couple and labile complex in excess ligand conditions." in the Supporting Information for details.

The characteristic time τ_d given by Eq. (9) can be physically interpreted as the exact time necessary to reach the accumulation for AGNES conditions (i.e. equilibrium with a gain $Y = 1/\theta$) if the supply is all the time in steady-state under diffusion-limited conditions [26]. This interpretation of τ_d given by (9) applies to reversible redox couples, but also to irreversible ones, because we are considering diffusion-limited conditions, and irreversibility is overcome at sufficiently negative deposition potentials (see pages 99–100 in ref. [27]). A graphical determination of τ_d is shown in Fig. 1.

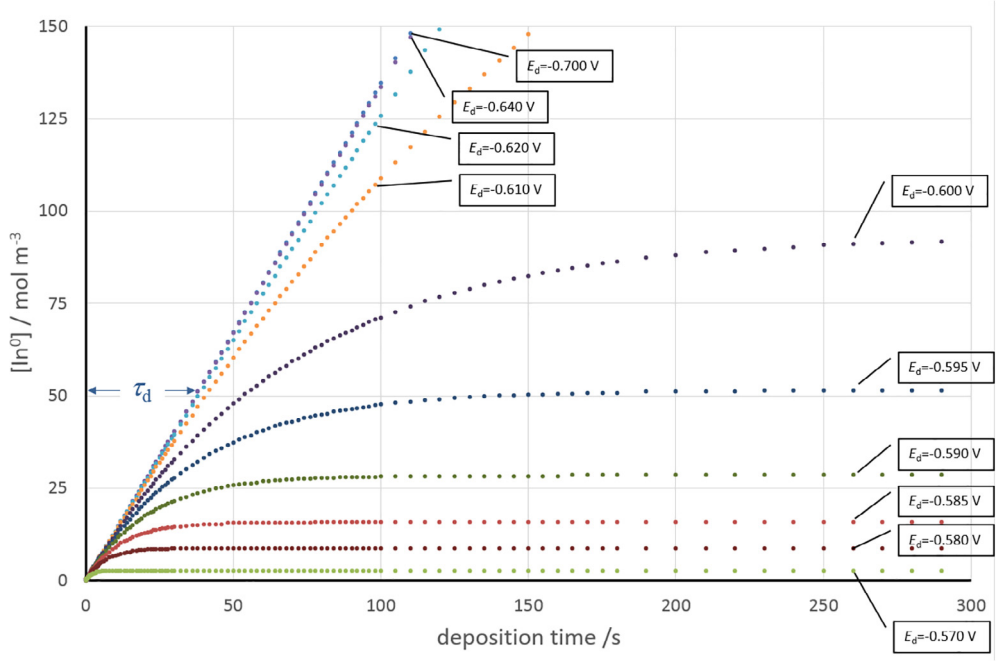

Fig. 1. Simulated accumulation evolution of the concentration of In° during one potential step at a fixed deposition potential (various markers in various series, see internal labels) using Eq. SI-10. One AGNES trajectory corresponds to one series, with the horizontal plateau indicating equilibrium. One SSCP wave fixes the deposition time (see vertical dashed line and circle markers) and scans the deposition potential, with the highest points corresponding to diffusion-limited conditions and the lowest points coincident with AGNES plateaus (see full circles). The shaded region corresponds to (approximate) equilibrium conditions for AGNES. The characteristic time τ_d for E_d = -0.595 V is also indicated. Simulation parameters for an RDE experiment (assuming full reversibility) are $E^\circ = -0.5075$ V, $n = 3$, $\upsilon = 10^{-6}$ m s^{-1}, $\omega = 157.079$ s^{-1}, $D_{In3+} = 1.55 \times 10^{-9}$ m^2 s^{-1}, $A = 10^{-6}$ m^2, $V_{Hg} = 1.2 \times 10^{-13}$ m^3, $[In^{3+}] = 5.0 \times 10^{-4}$ mol m^{-3}.

The factor $(1 + K')$ in Eq. (9) also illustrates how the complexes' contribution to the flux reduces the minimum required deposition time in AGNES [11,28]. See section "Time to reach AGNES conditions" in the Supporting Information for details. Eq. (9) also indicates that the larger the area-to-volume ratio of the electrode (for a fixed shape and gain), the faster AGNES equilibrium can be reached. So, achieving a huge gain with the largest drop of the HMDE (Hanging Mercury Drop Electrode) can take of the order of 1000 times longer than with the Thin Film-Rotating Disc Electrode, RDE [9]. RDE consists in a large assembly of hemispherical Hg nanodrops; their diffusion layers overlap and diffusion becomes essentially planar, with a large effective area to volume ratio. The required deposition times in RDE are also short due to the enhanced mass transport forced by the electrode rotation.

In each SCP experiment, the number of moles reduced at the working electrode during the deposition step equals the number of moles reoxidized during the stripping step. Thus, it has been found that, regardless of the reversibility of the electrodic reaction,

$$\tau = \frac{I_d^* \tau_d}{I_s}\left[1 - \exp\left(-\frac{t_d}{\tau_d}\right)\right] \quad (11)$$

holds in simple solutions, with τ_d given by various expressions according to the considered phenomena [29]. Notice that for sufficiently negative deposition potentials, I_d^* is given by Eq. (5), because the heterogeneous reaction is no longer the limiting step.

The region "foot of the wave" was already recognized as fostering equilibrium in the presentation of SSCP fundamentals [20,30] and in pseudopolarography [31,32]. If the applied potential is not too negative (i.e. one is asking for a moderate gain), so that t_d is long enough for equilibrium attainment, the SSCP point will be equivalent to an AGNES run [14,26,33]. So, some points in the foot of the SSCP wave could be under AGNES conditions.

The fact that some SSCP points can also fulfill AGNES conditions is illustrated in the simulations of the expected In° accumulation (in a RDE) with increasing deposition time shown in Fig. 1. Indeed, each series (corresponding to one fixed deposition potential along the increasing deposition times) can be considered as an AGNES trajectory (because the measured charge in the second stage is always proportional to the concentration of In° accumulated in the first stage), where the stabilization of the plateau occurs at longer times when the deposition potential becomes more negative (i.e. higher gains). An SSCP wave can be considered as the collection of points at a given deposition time (e.g. $t_d = 100$ s is shown in dashed line in the figure). Notice how the lowest points in this vertical dashed line (i.e. SSCP points) belong also to plateaus of the trajectories (i.e. fulfill AGNES conditions).

3. Materials and methods

3.1. Batch preparation

All the solutions used for the experiments were prepared with ultrapure water (18.2 MΩ cm, Elga labwater). In(III) solutions were obtained from dilution of a 1000 mg L^{-1} certified standard solution (Fluka). The ionic strength of the indium solution was fixed at 25 mmol L^{-1} with sodium perchlorate ($NaClO_4$) (Fluka, ≥98%). Perchloric acid ($HClO_4$) (Fluka) or sodium hydroxide (NaOH) (Merck suprapur) solutions were used to adjust solution pH. Total indium concentrations were set at 50 nmol L^{-1} or 25 nmol L^{-1} at pH = 2.5, 3.0, 3.5 or 4.0. Prepared solutions were equilibrated at least for 24 h prior to the measurements. During electroanalytical measurements, oxygen elimination in the solution batches was performed using Nitrogen (>99.999% pure) purchased from Air Liquide. All experiments were carried out at 25 °C using a thermostatic bath.

3.2. Electrochemical measurements

An Ecochemie Autolab type III potentiostat controlled by GPES 4.9 software (Ecochemie, The Netherlands) was used in conjunction with a

Metrohm 663VA stand. The electrochemical set up was composed of 3 electrodes. The reference electrode was a Ag/AgCl (in KCl) Dri-ref-5 electrode from WPI (Sarasota, FL, U.S.A.), the counter-electrode was a glassy carbon electrode and the working electrode was a thin mercury film plated onto a rotating glassy carbon disk of 2 mm diameter (Metrohm) as detailed hereafter.

The detailed protocol is based on the work published by Monterroso *et al.* [34]. The first step consists in polishing the electrode surface using alumina (Metrohm) slurry for 1 min, followed by a thorough washing with ultrapure water and ethanol. Then, an electrochemical pre-treatment of 50 successive cyclic voltammograms between −0.8 and + 0.8 V at 0.1 $V.s^{-1}$ in NH_4Ac 1 M/HCl 0.5 M solution is performed. The third step is the electrodeposition of the thin Hg film onto the glassy carbon surface. The electrode is placed in a Hg(II) solution 0.32 mmol L^{-1} (pH 1.9) and deposited using a potential of −1.3 V for a period of 420 s using a rotation rate of 1000 rpm. After each working day, the charge associated with the deposited Hg was determined to assess the state of the mercury film. This was carried out by electronic integration of the linear sweep stripping peak of Hg with a scan rate v = 0.005 V s^{-1} in 5 mmol L^{-1} of ammonium thiocyanide (pH 3.4) using a stripping range from −0.150 V to +0.400 V. From the measured Hg charges and using Faraday's law and the volumic mass of mercury, the Hg volume V is estimated at 4.11 × 10^{-13} m^3 (3% RSD) [35]. The preparation of the rotating disk/thin mercury film electrode was repeated daily for each set of experiments. Rocha *et al*, [35] reported that at least 60 SCP measurements can be performed without electrode degradation. In recent overnight tests for SCP and AGNES, we observed that up to 160 measures could be carried out without electrode degradation, which is largely sufficient for one day work.

3.3. SSCP measurements.

Metal deposition step at the mercury electrode was achieved by applying different values of potential E_d for a given deposition time (t_d) under agitation conditions (1000 rpm rotation speed or ω = 157 s^{-1}). For our experimental conditions, E_d varied between −0.5300 V and −0.6700 V vs Ag/AgCl and t_d between 45 s and 180 s. For the stripping step, the oxidizing current was fixed at I_s = 3 μA.

3.4. AGNES trajectories

The trajectories were performed for deposition potentials −0.5750 V and –0.5800 V, by varying the deposition time from 10 s to 300 s, for a solution containing a total indium concentration of 50 nmol L^{-1} at pH 3.5. For the stripping step, the oxidizing current was also set at 3 μA.

4. Results and discussion

4.1. AGNES trajectories and Nernstian equilibrium

A time-course experiment, where the response function (for instance, the stripped charge) is plotted against the deposition times, is typically called "trajectory" in AGNES literature. If a trajectory reaches a final plateau (i.e. stabilization for longer deposition times), it implies that equilibrium has been attained. Indeed, when –for instance- the stripped charge Q does not increase despite increasing the deposition time, it means that the deposition process has ceased due to the fulfillment of equilibrium, including the electrodic process (see section "Time to reach AGNES conditions" in the SI for details). This attainment of equilibrium can be seen in an indium solution in Fig. 2A (see also Fig. 3A in ref. [9] with RDE or Fig. 4a in ref. [10] with HMDE).

The proportionality between Q (of the plateau) and Y indicates the Nernstian equilibrium, i.e. fulfillment of Eq. (2). This proportionality is clearly seen in the collapse of the normalized trajectories of Fig. 2B when Q/Y is plotted vs (deposition time)/Y (see also Fig. 3B in ref. [9] or Fig. 4b in ref. [10]) or in dedicated plots Q vs Y (see Fig. 4 in ref. [9]).

Actually, rigorous AGNES conditions by the end of the deposition stage require equilibrium in all the homogeneous and heterogeneous processes in which the target species can participate (i.e. simultaneous equilibria). Given the presence of indium hydroxy complexes, in the case of In, at least 3 equilibria are required: a) In^{3+}/In°, b) In^{3+} with its hydroxy species and c) In° with In(III) hydroxy species. As In(III) hydroxy species display electrochemically reversible behaviour [14], one can expect equilibrium c) to be reached in an experimentally accessible time. On the other hand, equilibrium b) is also fast, in accordance to the reported high lability of these complexes in solution [14]. But, due to thermodynamic consistency, whenever equilibria c) and b) hold, also equilibrium a) does [9]. See section "SSCP model for irreversible redox couple and fully labile (reversible electroactive) complex in excess ligand conditions." in the SI for a particular modelled case. The physical dynamic picture can be described as: i) In° is mostly supplied to the amalgam from the reduction of the In(III) hydroxy species (due to the irreversibility of In^{3+} reduction, [14]); ii) any deple-

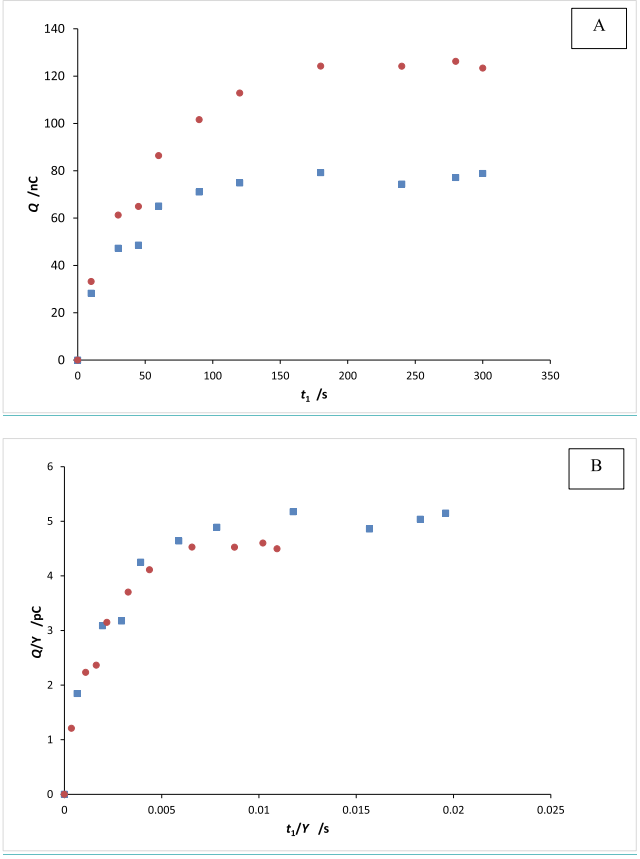

Fig. 2. Trajectories for AGNES with the RDE (panel A) and collapse of their normalized trajectories (panel B) indicating Nernstian behaviour of AGNES response in an indium solution. pH 3.5, t_1 = 90 s, $c_{T,In}$ = 5 × 10^{-8} mol L^{-1}. Markers for different deposition potentials (and gains): blue square marker, –0.575 V (Y = 15306); red circle marker, – 0.580 V (Y = 27444). Gains were computed using Eq. (9) in ref.This image should be deleted as it was a Marked Change (of the removed image) [10] with data from a calibration at pH 3.5 with E_{calib} = −0.570 V which corresponded to Y_{calib} = 8537. (For interpretation of the references to colour in this figure legend, the reader is referred to the web version of this article.)

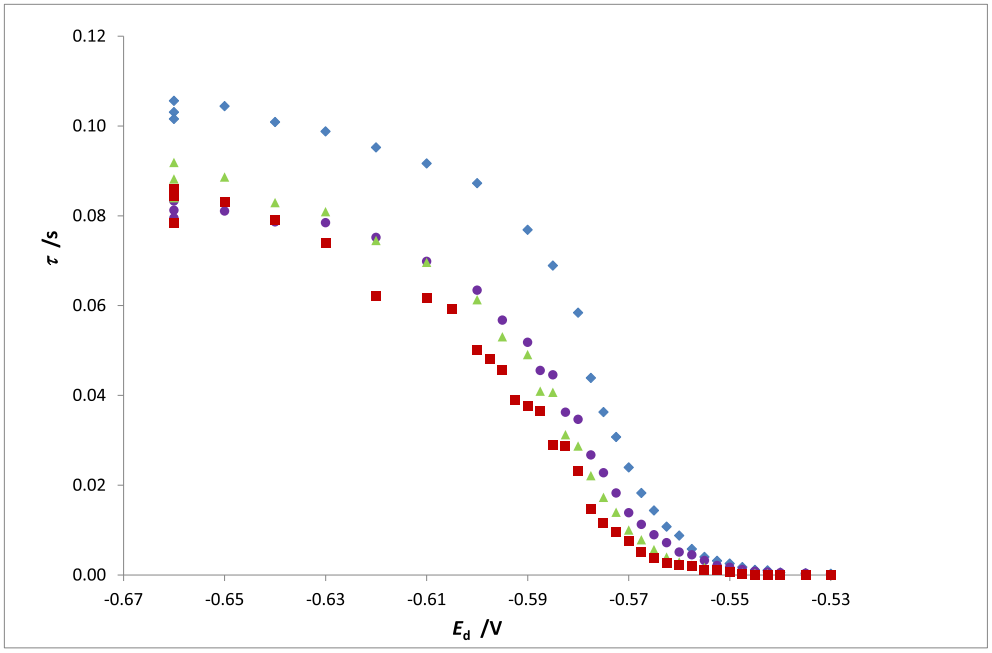

Fig. 3. Classical representation of SSCP waves in indium solutions with $c_{T,In} = 5 \times 10^{-8}$ mol L^{-1}; $t_d = 90$ s. Blue diamonds stand for pH 2.5; purple bullets for pH 3.0; green triangles for pH 3.5 and red squares for pH 4.0. (For interpretation of the references to colour in this figure legend, the reader is referred to the web version of this article.)

tion (and replenishment) of these complexes is also mimicked by the In^{3+} profile (due to lability) and iii) eventually the required In° concentration is reached with all other In(III) species in equilibrium. In these conditions, it does not matter which species has or have transported the required In(III) and suffered the electrodic process to accumulate a given amount of In°, the deposition potential controlling the eventual concentration ratios In^{3+}/In° and In (III) hydroxides/In°. Thus, equilibrium In^{3+}/In° is compatible even with a hypothetical total In^{3+}irreversibility at the electrode, whenever In(III) hydroxides are electroactive, by providing the concentration of In° required by the Nernst equilibrium at the potential considered within a reasonable deposition time. The shift of the electrodic wave towards more negative deposition potential values (in a dynamic technique, such as SSCP) as pH increases reflects the In(III) hydroxy species/In° equilibrium ratio and impacts on the time required to reach equilibrium at a given deposition potential, but this could not prevent eventual equilibrium measurements. Clearly, AGNES is an equilibrium technique being immaterial the way how this equilibrium is reached and the same applies to the potential range in the foot of the wave of SCCP experiments where equilibrium by the end of the deposition step is reached (see Section 4.2). In typical applications of AGNES one checks: A) the stabilization of trajectory at (at least) one gain; B) the Nernstian relationship between response functions at (at least) two gains.

Some systems, in the published literature, where [In^{3+}] has been measured, are:

- Speciation with NTA [10] confirmed with results from ref. [36]
- Speciation with oxalate [10,11], confirmed with results from ref. [37]
- pH impact on [In^{3+}] [9], confirmed with stability constants reported in ref. [38]
- $In(OH)_3$ solubility product (from pH 4 to 6) [11] agreeing with the database NIST 46.7, reaching concentrations in the pmol L^{-1} range.

The impact of the irreversibility of the redox couple In^{3+}/In° on AGNES in these works was: i) the unsuitability of Differential Pulse Polarography to compute the gain associated to a given deposition potential (so the gain is obtained from a calibration), and ii) a slightly larger minimum time to reach equilibration in solutions with no added ligand ("rule of thumb" of ten times the gain, instead of seven times as in Zn, Cd and Pb when using HMDE, smallest drop 1) [10].

AGNES has encountered poorly reversible systems in the determination of Zn^{2+} in complex matrices (wine [39], ZnO nanoparticles with adsorbing dispersant [40], etc.). The usual practical strategy (to diagnose and overcome irreversibility) has been to use the variant AGNES-2P, where a first sub-stage under diffusion-limited conditions is inserted to accumulate an important fraction of the needed amount of Zn^0 in a short time. In these cases, the relaxation towards equilibrium in dedicated trajectories is very slow even for small gains. This slow relaxation for small gains has not yet been seen in an indium system.

As further proof that AGNES is not hindered by indium irreversibility, we are going, in the rest of this article, to show that AGNES conditions can be met at the foot of SSCP waves in indium solutions.

4.2. Visualization of AGNES regime in an SSCP wave

4.2.1. Mathematical basis of the new visualization

Fig. 3 shows the classical representation of some SSCP experimental waves in indium solutions measured with RDE.

There might be a region of the foot of the wave (in this classical representation), where τ values become independent of t_d (see Fig. 3 in ref. [20]), because equilibrium has been attained within this t_d. This is expected to happen when $t_d \gg \tau_d$. In this AGNES region, τ can be computed from the equilibrium expression:

$$\tau = \frac{3FV\left[In^{3+}\right]}{(I_s - I_{Ox})\theta} \tag{12}$$

(which can be seen as just as a recasting of Eq. (2)).

At the other extreme of the wave, under diffusion-limited conditions, τ^* can be computed from I_d^* given by Eq. (5),

$$\tau^* = \frac{I_d^* t_d}{(I_s - I_{Ox})} = \frac{3FAD_{In^{3+}}(1 + \varepsilon K')\left[In^{3+}\right]t_d}{(I_s - I_{Ox})\delta} \tag{13}$$

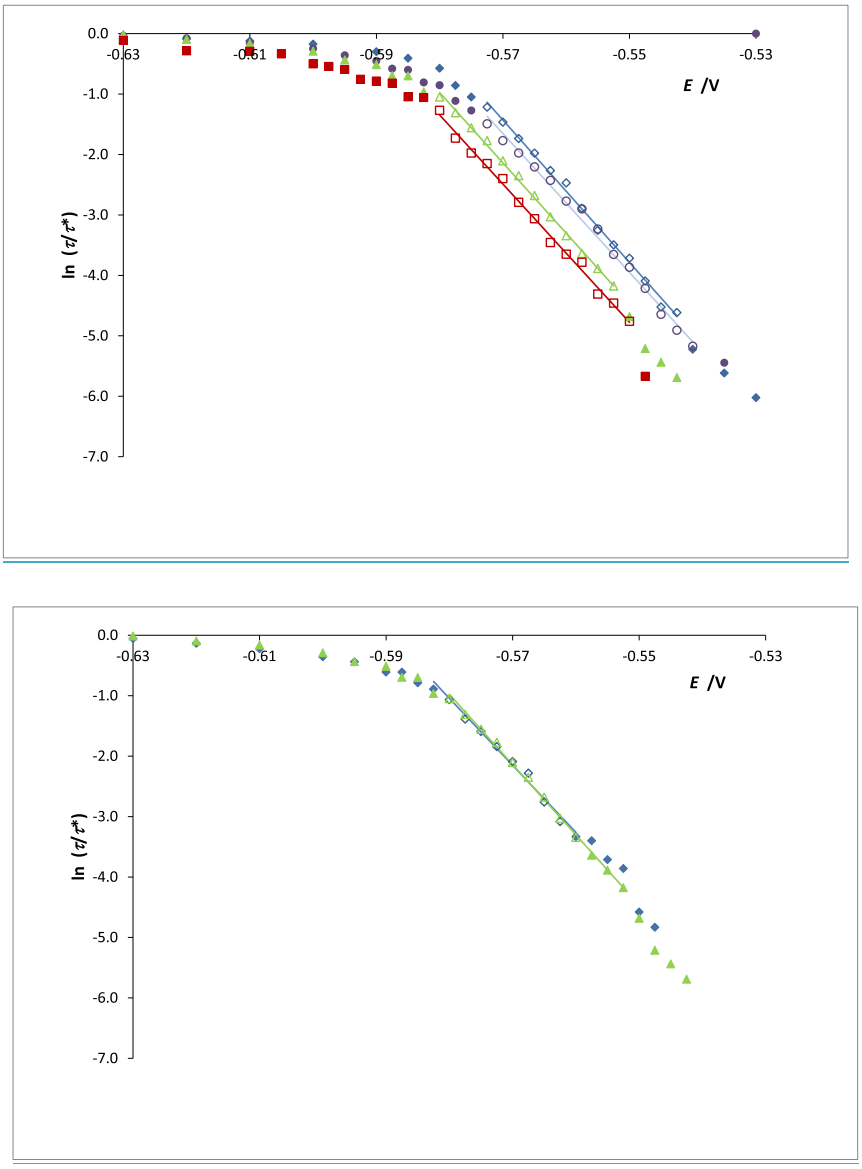

Fig. 4. Visualization of the AGNES regime in SSCP waves recognized as straight segments (with regression lines of slope close to -3*F*/*RT*). Open markers indicate when AGNES conditions are fulfilled. Same data, markers and conditions as in Fig. 3.

where full lability of the complexes has been assumed. Other assumptions are as those around Eq. (5).

Combining previous expressions, one obtains

$$\ln\left(\frac{\tau}{\tau^*}\right) = \ln\left(\frac{V\delta}{AD_{In^{3+}}(1+\varepsilon K')t_d}\right) + \frac{3F}{RT}E^{0'} - \frac{3F}{RT}E_d \qquad (14)$$

This equation holds in the indium system (even if the redox couple In^{3+}/In° was fully irreversible) because:

i) τ corresponds to an equilibrium situation where no kinetic parameter is relevant (see previous section).
ii) τ* corresponds to diffusion-limited conditions when irreversibility is overcome (e.g. τ_d given by Eq. (9) applies).

4.2.2. The linear region of the new visualization indicates AGNES conditions

Fig. 4 shows a new visualization of SSCP results, inspired by Eq. (14) and by Fig. 7 in ref. [28], where ln (τ/τ*) vs E_d is plotted. This visualitzation is equivalent to pseudopolarograms in logarithmic scale for ordinates (see Figs. 1b and 3b in ref. [31] or Figs. 4b and 6b in ref. [32]). The plotting of ln (τ/τ*) vs E_d is more suitable than the "polarographic logarithmic analysis" (i.e. plotting log (τ/(τ-τ*)) vs E_d) to diagnose AGNES conditions in SSCP or pseudopolarography, because the "polarographic logarithmic analysis" would also show a straight line in regions where there is not "absence of gradients in the concentration profiles". For instance the plotting of log (τ/(τ-τ*)) vs E_d with the data of Fig. 1 (e.g. at t_d = 100 s, see Fig SI-3) would result in a straight line for ALL the points (e.g. including E_d = −0.640 V, where one is close to diffusion-limited conditions, far away from the foot of the wave), because the electrodic reaction has been assumed as fully reversible. This linearity beyond AGNES conditions in polarographic logarithmic analysis can be seen, for experimental results, in the inset of Fig. 5a of ref. [31].

One can identify in Fig. 4 at least twelve AGNES points (open markers) for each pH, defining practically parallel lines. The expected slope (of the Nernstian segment) for a system exchanging 3 electrons should approach $-118.8\ V^{-1}$ (regardless of electrodic irreversibility), as seen in Eq. (14). The slopes in Fig. 4 are −118 ± 2, −115 ± 3, −116 ± 2 and $-114 \pm 2\ V^{-1}$ (for increasing pH values), which might be seen as

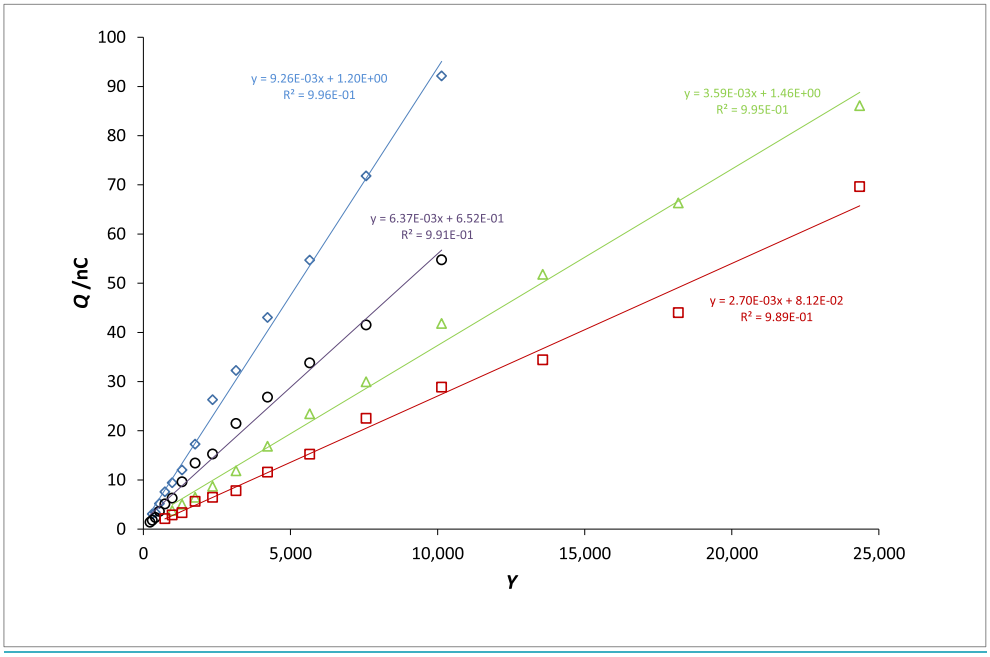

Fig. 5. AGNES charges from the recognized points used in Fig. 4 for different gains. The linearity confirms Nernstian behaviour. A common $E^{\circ\prime}$ = –0.5019 V (see section 4.2.2) was used for all series. Same markers and conditions as in Fig. 4.

an acceptable scattering. Thus, the linear region in the ln (τ/τ^*) vs E_d plot (Fig. 4) indicates AGNES conditions (i.e. Nernstian equilibrium) in this *indium* system.

The linear segment in the new representation is equivalent to the typical AGNES Q vs Y plots (see Fig. 5 with the same data as in Fig. 4 or Fig. 4 in ref. [9]), because it is just a consequence of Nernst law. As expected from Eq. (2) and the fact that η_Q is fixed (from the fixed volume of deposited Hg in the RDE, see Eq. (3), the steepest slope in the plot Q vs Y corresponds to the highest [In^{3+}] (i.e. to the lowest pH). In Fig. 5, the gains have been computed by using $E^{0\prime}$ from the average of all $(E^{0\prime})_j$ which are found from the points in the linear segment in the new visualization of SSCP waves. Indeed, Eq. (1) in combination with Eqs. (2) and (4), can be re-written as

$$\left(E^{0'}\right)_j = E_{d,j} + \frac{RT}{3F}\ln\left(\frac{\tau_j(I_s - I_{Ox})}{\left[In^{3+}\right]3FV}\right) \quad (15)$$

where the index j runs along each of the points in the linear segment (e.g. $E_{d,3}$ is the deposition potential of the third point in the linear segment). From the average of $(E^{\circ\prime})_j$, one finds $E^{\circ\prime}$ which gives access to the assignment of a gain for any associated deposition potential *via* Eq. (1). From the data in Fig. 4, we obtained $E^{\circ\prime}$ −0.4892, −0.4923, −0.4964 and −0.4963 V (for increasing pH values), and worked with their average −0.4935 V in the building up of Fig. 5.

A fixed deposition potential implies a fixed gain Y, regardless of pH (see Eq. (1)). For the fixed deposition time of 90 s, AGNES conditions have been reached in Fig. 4 for the two highest pH-values at E_d = −0.580 V, but this t_d has not been sufficient for pH = 2.50 or pH = 3.04 (for the low pH values, the more negative potential with achievable equilibrium in 90 s is −0.5725 V). So, one concludes that the linear Nernstian region of SSCP waves in these indium solutions is more extense (i.e. wider deposition potential range) for higher pH, as expected from the increased contribution of the hydroxy complexes [11,26,28], because of both, their (very high, but probably not full) lability and their electroactivity [14].

4.2.3. Properties of the linear regions of the new visualization

a) The linear range (in E_d) is longer (i.e. linearity starting at a more negative E_d) for longer t_d (also the intercept is affected).
A longer t_d is a longer t_1 in AGNES nomenclature, and allows for equilibrium to be reached even with higher gains. Unfortunately, this effect cannot be seen in Fig. 6, probably because of the relatively short deposition times used in this case. On the other hand, one does see that the intercept of the lines shifts towards lower values on the ordinate axis with increasing t_d, which is intuitively understood as τ not being changed (due to equilibrium), but τ^* being proportional to t_d (see, for instance, Eq. (13)). This property was earlier described for pseudopolarography [31], as well as the fact that smaller electrodes facilitate equilibrium conditions (as in AGNES [1]).

b) The linear region is independent of total In concentration (under fixed total-to-free concentration ratio 1 + K').
As seen in Eq. (14), the total concentration of indium does not impact on the quotient τ/τ^*. Keeping a fixed pH, implies a fixed K', so free and total concentrations are in a fixed ratio. τ is proportional to the free indium concentration, while τ^* is proportional to $(1 + \varepsilon K')\left[In^{3+}\right]$ (we are assuming full lability; otherwise we should include the lability degree [41,42]) times the free indium concentration. Thus, the free concentration dependence cancels out. This expected collapse of the lines in the new visualization can be seen in Fig. 7. The lack of shift of the Nernstian region with changing total concentration was already described for pseudopolarography [31].

We turn now our attention towards whether increasing the total concentration modifies the required time to reach AGNES equilibrium. It is well known in AGNES, that –for solutions without metal complexation- the equilibrium time is proportional to the gain, but independent of the free metal concentration. Indeed, if the free concentration increases by a factor g, there will be an increase in the

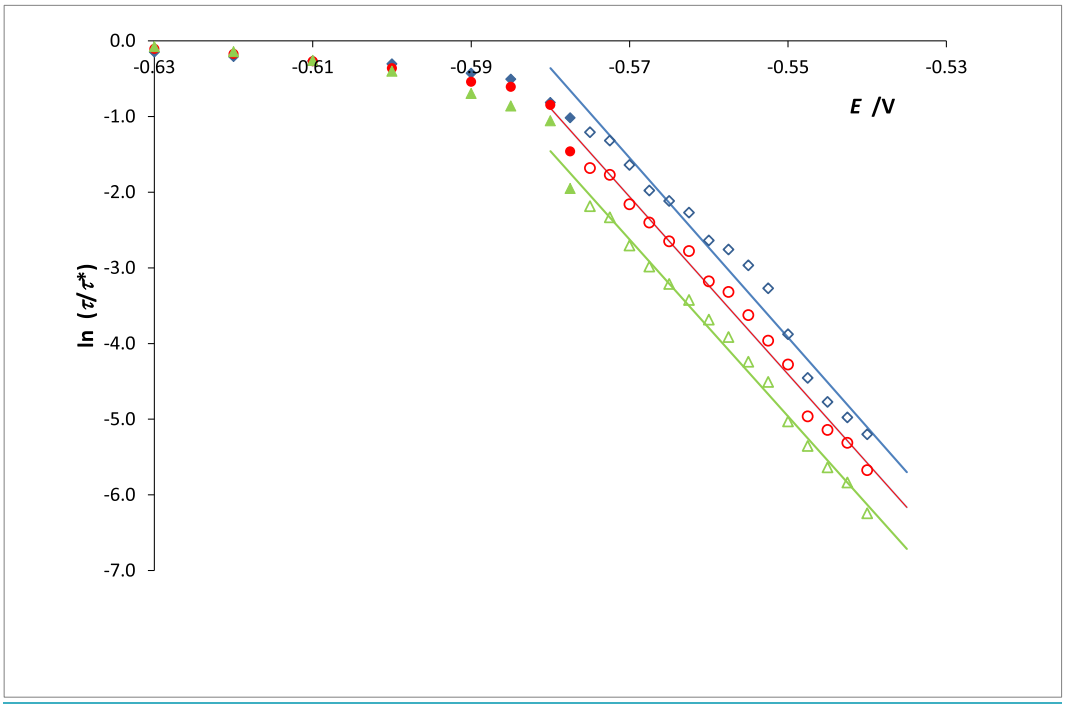

Fig. 6. Impact of the deposition time on the AGNES-regime visualization plot. Blue diamonds stand for t_d = 45 s; red circles for t_d = 90 s and green triangles for t_d = 180 s. $c_{T,In} = 5 \times 10^{-8}$ mol L^{-1}; pH = 3.5. (For interpretation of the references to colour in this figure legend, the reader is referred to the web version of this article.)

flux by this factor *g*, but also in the amount of required In°. In solutions with metal complexation, there is a reduction of the required deposition time by another factor $f = (1 + \varepsilon K'\xi)$ where ξ is the so-called lability degree (which is unity when assuming full lability), but the same factor *f* applies at all indium concentrations (due to fixed pH), so there is no variation in the potential range of linearity in the visualization plot. This is consistent with data shown in Fig. 7.

4.2.4. Missing linear AGNES-region in the new visualization

We caution that for other systems (other metals and/or other matrices), where there was not a significant fraction of the metal in solution as an electroactive species, the used t_d might be too short for the SSCP wave to exhibit any perceivable linear segment in the proposed new visualization. In this respect, it is convenient not to identify "foot of the wave" (which can be arbitrarily defined) with "AGNES region" (which might or might not be seen in the available data).

Unless all relevant species in the system were totally irreversible close to the standard redox potential, a sufficiently long deposition time should lead to the Nernstian linear segment (especially with large area-to-volume electrodes). In other words: except for total irreversibility with no electroactive complex, there is a sufficiently less negative potential (i.e. low enough gain) for which a given t_d is sufficient to reach equilibrium, but the corresponding τ might be too small to be accurately measured. If the AGNES region is not seen with a certain t_d, a first recommendation in order to try to emerge it is to increase this t_d.

See section "SSCP model for irreversible redox couple and fully labile (reversible electroactive) complex in excess ligand conditions." in the SI, for details on how irreversibility of one species in fast equilibrium with a reversible species does not impact on the SSCP wave.

4.2.5. Other indicators of AGNES conditions in the foot of an SSCP wave

Another visualization of AGNES conditions being fulfilled at the foot of wave is the clustering of processed points when the SSCP wave is analyzed with the mathematical treatment that transforms SSCP individual points in pairs of metal and complex concentrations at the electrode surface [33,43].

4.3. Extension to other cases

The previous discussion on the application of AGNES to the [In^{3+}] measurement illustrates a particular case of a system where an element X coexists with some complex XL, one of these species or both being electroactive. Several cases can be discussed:

4.3.1. X is electroactive, XL is not electroactive

This is the typical case for many elements: X is electrochemically reversible (or quasi-reversible), while XL is not electroactive. We first consider the case where the initial bulk concentrations of X and XL are in equilibrium. The measurement of [X] requires the equilibrium X/X°, which in turn, implies the full equilibrium XL/X/X°. The kinetics of the interconversion XL/X just increasingly help in the supply of X to be reduced at the electrode surface as the rate of interconversion XL/X increases. If the initial conditions do not correspond to equilibrium X/XL in the bulk, the reaching of equilibrium X/X° will be influenced by the time dependence of the X concentration as determined by the kinetics of interconversion X/XL. The concentration of X measured will, then, be different from the initial one (in the bulk) and dependent on the time scales of the processes X/X° and X/XL. If the reduction of X is possible, but very slow, the achievement of the equilibrium X/X° could be delayed beyond a given practical experimental time.

4.3.2. X is not electroactive, XL is electroactive

We first consider the case where the initial bulk concentrations of X and XL are in equilibrium. If the electroactive species is XL, the equilibrium X/X° and the measurement of [X] could still be reached through the reduction of XL. If the initial bulk concentrations X/XL are not in equilibrium, the measured [X] will be influenced by the time scales of the kinetics of the X/XL and XL/X° processes. If the reduction

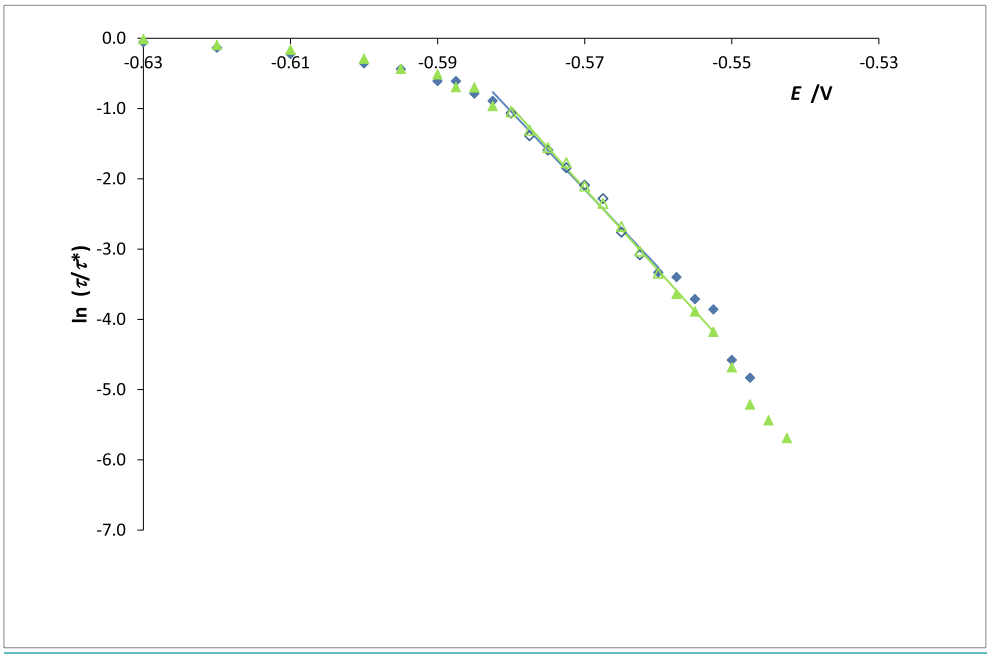

Fig. 7. Impact of the total concentration of indium on the AGNES-regime visualization plot. Blue diamonds stand for $c_{T,In} = 2.5 \times 10^{-8}$ mol L^{-1}, while green triangles for $c_{T,In} = 5 \times 10^{-8}$ mol L^{-1}. $t_d = 90$ s and pH = 3.5. (For interpretation of the references to colour in this figure legend, the reader is referred to the web version of this article.)

of XL is slow, the achievement of the equilibrium X/X° could lie beyond a given experimental time.

4.3.3. Both, X and XL are electroactive

This case can be seen as a superposition of both cases above outlined.

5. Conclusions

Free indium concentrations can be obtained from AGNES measurements, as experimentally found in systems containing NTA, oxalate, precipitated indium hydroxide, etc. Irreversibility of the redox couple In°/In^{3+} is relevant for the much shorter timescale of the DPP technique, which is avoided by a suitable AGNES calibration given that the volume of the electrode is known. The lack of a relevant impact of In°/In^{3+} irreversibility on AGNES can be rationalized invoking the high lability and mobility of the hydroxy complexes, as well as their (partial or full) reversibility at the electrode.

AGNES conditions can also appear in points of the foot of an SSCP wave. This AGNES region can be visualized as a straight line in a plot of ln (τ/τ^*) *versus* the deposition potential, as seen in the indium case. This method can be applied to any element suitable for AGNES and its free concentration can be obtained from sufficiently accurate points in this region of the SSCP wave.

CRediT authorship contribution statement

Josep Galceran: Methodology, Writing – original draft. **Encarna Companys:** Visualization, Writing – review & editing. **Jaume Puy:** Conceptualization, Writing – review & editing. **Jose Paulo Pinheiro:** Methodology, Writing – original draft. **Elise Rotureau:** Investigation, Writing – review & editing.

Declaration of Competing Interest

The authors declare that they have no known competing financial interests or personal relationships that could have appeared to influence the work reported in this paper.

Acknowledgements

J.G., E.C. and J.P. gratefully acknowledge support for this research from the Spanish Ministry of Science and Innovation (MCIN/AEI/10.13039/501100011033 Project PID2019-107033GB-C21).

Appendix A. Supplementary data

Supplementary data to this article can be found online at https://doi.org/10.1016/j.jelechem.2021.115750.

References

[1] J. Galceran, E. Companys, J. Puy, J. Cecília, J.L. Garcés, AGNES: a new electroanalytical technique for measuring free metal ion concentration, J. Electroanal. Chem. 566 (2004) 95–109.
[2] E. Companys, J. Galceran, J.P. Pinheiro, J. Puy, P. Salaün, A review on electrochemical methods for trace metal speciation in environmental media, Curr. Opin. Electrochem. 3 (1) (2017) 144–162.
[3] W.B. Chen, C. Gueguen, D.S. Smith, J. Galceran, J. Puy, E. Companys, Metal (Pb, Cd, and Zn) binding to diverse organic matter samples and implications for speciation modeling, Environ. Sci. Technol. 52 (7) (2018) 4163–4172.
[4] M. Diaz-de-Alba, M.D. Galindo-Riano, J.P. Pinheiro, Lead electrochemical speciation analysis in seawater media by using AGNES and SSCP techniques, Environ. Chem. 11 (2) (2014) 137–149.
[5] R.M. Town, H.P. van Leeuwen, Intraparticulate speciation analysis of soft nanoparticulate metal complexes. The impact of electric condensation on the binding of $Cd^{2+}/Pb^{2+}/Cu^{2+}$ by humic acids, PCCP 18 (15) (2016) 10049–10058.
[6] R.M. Town, H.P. van Leeuwen, Intraparticulate metal speciation analysis of soft complexing nanoparticles. The intrinsic chemical heterogeneity of metal-humic acid complexes, J. Phys. Chem. A 120 (43) (2016) 8637–8644.

[7] R.F. Domingos, S. Carreira, J. Galceran, P. Salaün, J.P. Pinheiro, AGNES at vibrated gold microwire electrode for the direct quantification of free copper concentrations, Anal. Chim. Acta 920 (2016) 29–36.
[8] P. Pla-Vilanova, J. Galceran, J. Puy, E. Companys, M. Filella, Antimony speciation in aqueous solution followed with AGNES, J. Electroanal. Chem. 849 (2019) 113334.
[9] E. Rotureau, P. Pla-Vilanova, J. Galceran, E. Companys, J.P. Pinheiro, Towards improving the electroanalytical speciation analysis of indium, Anal. Chim. Acta 1052 (2019) 57–64.
[10] M.H. Tehrani, E. Companys, A. Dago, J. Puy, J. Galceran, Free Indium concentration determined with AGNES, Sci. Total Environ. 612 (2018) 269–275.
[11] M.H. Tehrani, E. Companys, A. Dago, J. Puy, J. Galceran, New methodology to measure low free indium (III) concentrations based on the determination of the lability degree of indium complexes. Assessment of In(OH)3 solubility product, J. Electroanal. Chem. 847 (2019) 113185.
[12] J.G. Lawson, D.A. Aikens, Mechanism and thermodynamics of polarographic deposition of aquo In(3), J. Electroanal. Chem. 15 (2–3) (1967) 193–1000.
[13] R.R. Nazmutdinov, T.T. Zinkicheva, G.A. Tsirlina, Z.V. Kuz'minova, Why does the hydrolysis of In(III) aquacomplexes make them electrochemically more active?, Electrochim Acta 50 (25–26) (2005) 4888–4896.
[14] R.M. Town, J.F.L. Duval, H.P. van Leeuwen, Electrochemical activity of various types of aqueous In(III) species at a mercury electrode, J. Solid State Electrochem. 24 (2020) 2807–2818.
[15] S. Inouye, H. Imai, Electrode kinetics of indium (III) at the dropping mercury electrode, Bull. Chem. Soc. Jpn. 33 (2) (1960) 149–152.
[16] E. Sahlin, D. Jagner, Calibration-free determination of copper, zinc, cadmium and lead in tap water using coulometric stripping potentiometry, Electroanalysis 10 (8) (1998) 532–535.
[17] N. Serrano, J.M. Diaz-Cruz, C. Arino, M. Esteban, Stripping chronopotentiometry in environmental analysis, Electroanalysis 19 (19–20) (2007) 2039–2049.
[18] R.M. Town, H.P. van Leeuwen, Fundamental features of metal ion determination by stripping chronopotentiometry, J. Electroanal. Chem. 509 (1) (2001) 58–65.
[19] C. Parat, L. Authier, D. Aguilar, E. Companys, J. Puy, J. Galceran, M. Potin-Gautier, Direct determination of free metal concentration by implementing stripping chronopotentiometry as second stage of AGNES, Analyst 136 (2011) 4337–4343.
[20] H.P. van Leeuwen, R.M. Town, Stripping chronopotentiometry at scanned deposition potential (SSCP). Part 1. Fundamental features, J. Electroanal. Chem. 536 (1–2) (2002) 129–140.
[21] R.M. Town, H.P. van Leeuwen, Stripping chronopotentiometry at scanned deposition potential (SSCP) - part 2. Determination of metal ion speciation parameters, J. Electroanal. Chem. 541 (2003) 51–65.
[22] M. Branica, D.M. Novak, S. Bubic, Application of anodic-stripping voltammetry to determination of state of complexation of traces of metal-ions at low concentration levels, Croat. Chem. Acta 49 (3) (1977) 539–547.
[23] M.S. Shuman, J.L. Cromer, Pseudo-polarograms - applied potential anodic stripping peak current relationships, Anal. Chem. 51 (9) (1979) 1546–1550.
[24] R.M. Town, H.P. van Leeuwen, Stripping chronopotentiometry at scanned deposition potential (SSCP): an effective methodology for dynamic speciation analysis of nanoparticulate metal complexes, J. Electroanal. Chem. 853 (2019).
[25] H.P. van Leeuwen, R.M. Town, Stripping chronopotentiometry at scanned deposition potential (SSCP). Part 4. The kinetic current regime, J. Electroanal. Chem. 561 (1–2) (2004) 67–74.
[26] G. Alberti, R. Biesuz, C. Huidobro, E. Companys, J. Puy, J. Galceran, A comparison between the determination of free Pb(II) by two techniques: absence of gradients and Nernstian equilibrium stripping and resin titration, AcA 599 (2007) 41–50.
[27] A.J. Bard, L.R. Faulkner, Electrochemical Methods. Fundamentals and Applications, Second ed., John Wiley & Sons Inc, New York, 2001.
[28] E. Companys, J. Cecília, G. Codina, J. Puy, J. Galceran, Determination of the concentration of free Zn^{2+} with AGNES using different strategies to reduce the deposition time, J. Electroanal. Chem. 576 (1) (2005) 21–32.
[29] R.M. Town, J.P. Pinheiro, R. Domingos, H.P. van Leeuwen, Stripping chronopotentiometry at scanned deposition potential (SSCP). Part 6: features of irreversible complex systems, J. Electroanal. Chem. 580 (1) (2005) 57–67.
[30] H.P. van Leeuwen, R.M. Town, Stripping chronopotentiometry at scanned deposition potential (SSCP) part 3. Irreversible electrode reactions, J. Electroanal. Chem. 556 (2003) 93–102.
[31] D. Omanovic, M. Branica, Pseudopolarography of trace metals. Part II. The comparison of the reversible, quasireversible and irreversible electrode reactions, J. Electroanal. Chem. 565 (1) (2004) 37–48.
[32] D. Omanovic, Pseudopolarography of trace metals. Part III. Determination of stability constants of labile metal complexes, Croat. Chem. Acta 79 (1) (2006) 67–76.
[33] N. Serrano, J.M. Díaz-Cruz, C. Ariño, M. Esteban, J. Puy, E. Companys, J. Galceran, J. Cecilia, Full-wave analysis of stripping chronopotentiograms at scanned deposition potential (SSCP) as a tool for heavy metal speciation: theoretical development and application to Cd(II)-phthalate and Cd(II)-iodide systems, J. Electroanal. Chem. 600 (2007) 275–284.
[34] S.C.C. Monterroso, H.M. Carapuça, J.E.J. Simão, A.C. Duarte, Optimisation of mercury film deposition on glassy carbon electrodes: evaluation of the combined effects of pH, thiocyanate ion and deposition potential, Anal. Chim. Acta 503 (2) (2004) 203–212.
[35] L.S. Rocha, J.P. Pinheiro, H.M. Carapuca, Evaluation of nanometer thick mercury film electrodes for stripping chronopotentiometry, Journal of Electroanalytical Chemistry, Journal of Electroanalytical Chemistry (2007) 37–45.
[36] T. Biver, R. Friani, C. Gattai, F. Secco, M.R. Tine, M. Venturini, Mechanism of indium(III) exchange between NTA and transferrin: A kinetic approach, J. Phys. Chem. B 112 (38) (2008) 12168–12173.
[37] E. Vasca, D. Ferri, C. Manfredi, L. Torello, C. Fontanella, T. Caruso, S. Orru, Complex formation equilibria in the binary Zn2+-oxalate and In3+-oxalate systems, DTr 13 (2003) 2698–2703.
[38] E.A. Biryuk, V.A. Nazarenko, R.V. Ravitskaya, Spectrophotometric determination of the hydrolysis constants of indium ions, Russ. J. Inorg. Chem. 14 (1969) 503–506.
[39] E. Companys, M. Naval-Sanchez, N. Martinez-Micaelo, J. Puy, J. Galceran, Measurement of free zinc concentration in wine with AGNES, J. Agric. Food. Chem. 56 (18) (2008) 8296–8302.
[40] J. Galceran, M. Lao, C. David, E. Companys, C. Rey-Castro, J. Salvador, J. Puy, The impact of electrodic adsorption on Zn, Cd or Pb speciation measurements with AGNES, J. Electroanal. Chem. 722–723 (2014) 110–118.
[41] J. Galceran, J. Puy, J. Salvador, J. Cecília, H.P. van Leeuwen, Voltammetric lability of metal complexes at spherical microelectrodes with various radii, J. Electroanal. Chem. 505 (1–2) (2001) 85–94.
[42] J. Puy, J. Galceran, Theoretical aspects of dynamic metal speciation with electrochemical techniques, Curr. Opin. Electrochem. 1 (1) (2017) 80–87.
[43] J.P. Pinheiro, J. Galceran, E. Rotureau, E. Companys, J. Puy, Full wave analysis of stripping chronopotentiometry at scanned deposition potential (SSCP): obtaining binding curves in labile heterogeneous macromolecular systems for any metal-to-ligand ratio, J. Electroanal. Chem. 873 (2020).